

## Measurements of high-brightness electron beam

H. Wang, J. Power, W. Liu, and W. Gai

### Introduction

The purpose of the experiment is to obtain the emittance of high-brightness electron beam from AWA test-stand beamline. In our experiment, we first choose three positions from AWA test-stand beamline. For each position, we measure the beam spot size, and then we use PARMELA to simulate beam dynamics along the beamline under the same conditions as the experiment. The rms. envelope from PARMELA simulation is used to fit the measured data, so the actual rms. transverse emittance of the beam can be estimated from simulation results when good matching of beam envelope is achieved.

### Experimental setup

The experimental work was carried out at AWA test-stand beamline. The electrons are produced and accelerated by AWA 1.5 cell photocathode L-band (1300 MHz) RF gun. The beamline schematic is shown in Fig 1.

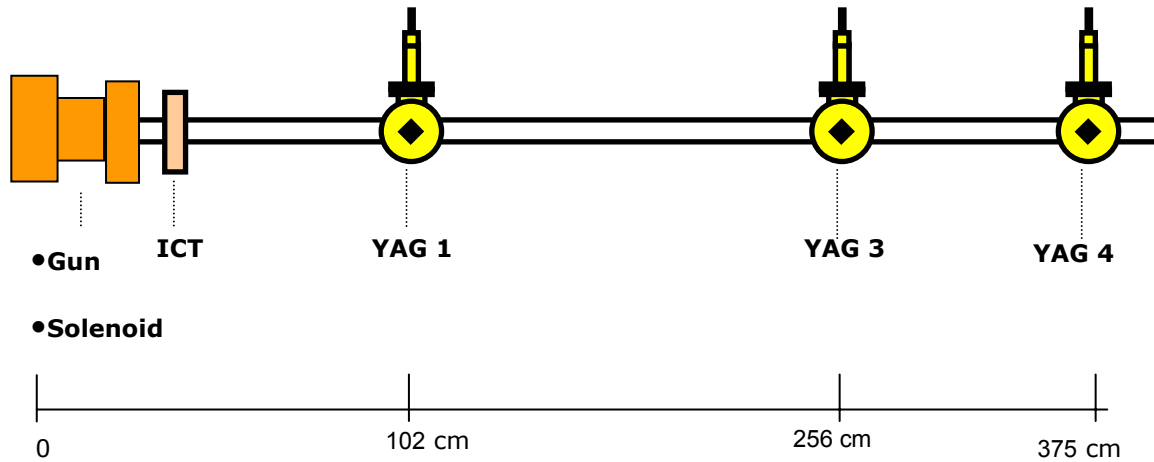


Fig. 1 Schematics of AWA test-stand beamline.

In this experiment three YAGs (YAG1, YAG3, and YAG4) are placed at three different positions along the beamline. The distance between YAG1 and cathode is 102cm, for YAG3 and YAG4 the distances are 256cm and 375cm respectively. For each YAG, there is a CCD camera to capture images. These cameras are carefully adjusted so that the captured images are located in the center of the cameras with high image resolution.

For each measurement we recorded original image, background image, and fiducial image. After all the measured data are put into image post-processor, we can obtain rms. beam spot sizes (rms. X and rms. Y). Due to the fluctuations of laser intensity and RF power, the charges of electron beams change in some range, so we recorded 30

images for each position, and then averaged the data to obtain mean rms. beam spot size at each position. (We will improve the measurement process in the future experiment by synchronizing laser output and RF power input to gun with image recording.)

## **Experiment results and analysis**

In this experiment we measured three groups of data, (1) Large laser spot size, (2) small laser spot size, and (3) high RF input power. The list of beam parameters is common for all 3 cases.

Laser pulse width = 8ps FWHM

For each group, laser fine delay (LFD), i.e. initial RF phase of gun, was varied, beam spots captured by CCD cameras from YAG1, YAG3, and YAG 4 were recorded. In the next three subsections, the measured data for each group will be shown and analyzed respectively.

### **1. Large laser spot size**

The measurement conditions used for this case are

R\_spot=1.425mm  
RF\_gun=215mV  
TSF=TSB=20000 counts  
TSM=27500 counts  
ICT=20-25mV (for LFD210)  
ICT=20-25mV (for LFD220)  
ICT=25-35mV (for LFD230)  
ICT=25-30mV (for LFD240)  
ICT=30-35mV (for LFD250)  
ICT=30-35mV (for LFD260)

Note:

“R\_spot” means radius of laser spot on photocathode.

“RF\_gun” means RF power input to gun.

“TSF” means test-stand focusing solenoid.

“TSB” means test-stand bucking solenoid.

“TSM” means test-stand matching solenoid.

In this subsection we varied laser fine delay (LFD) from 210 to 260. The typical images of beam spots at YAG1, YAG3, and YAG4 are shown in Fig. 2, these images have been processed, and the background noises were removed. Table 1 shows rms. X (horizontal direction) and rms. Y (vertical direction) of beam spots for the three positions, since the measured beam spots were elliptic, not round, rms. R (geometric mean of rms. X and rms. Y) was calculated, and listed in the table for easy comparison to PARMELA simulation.

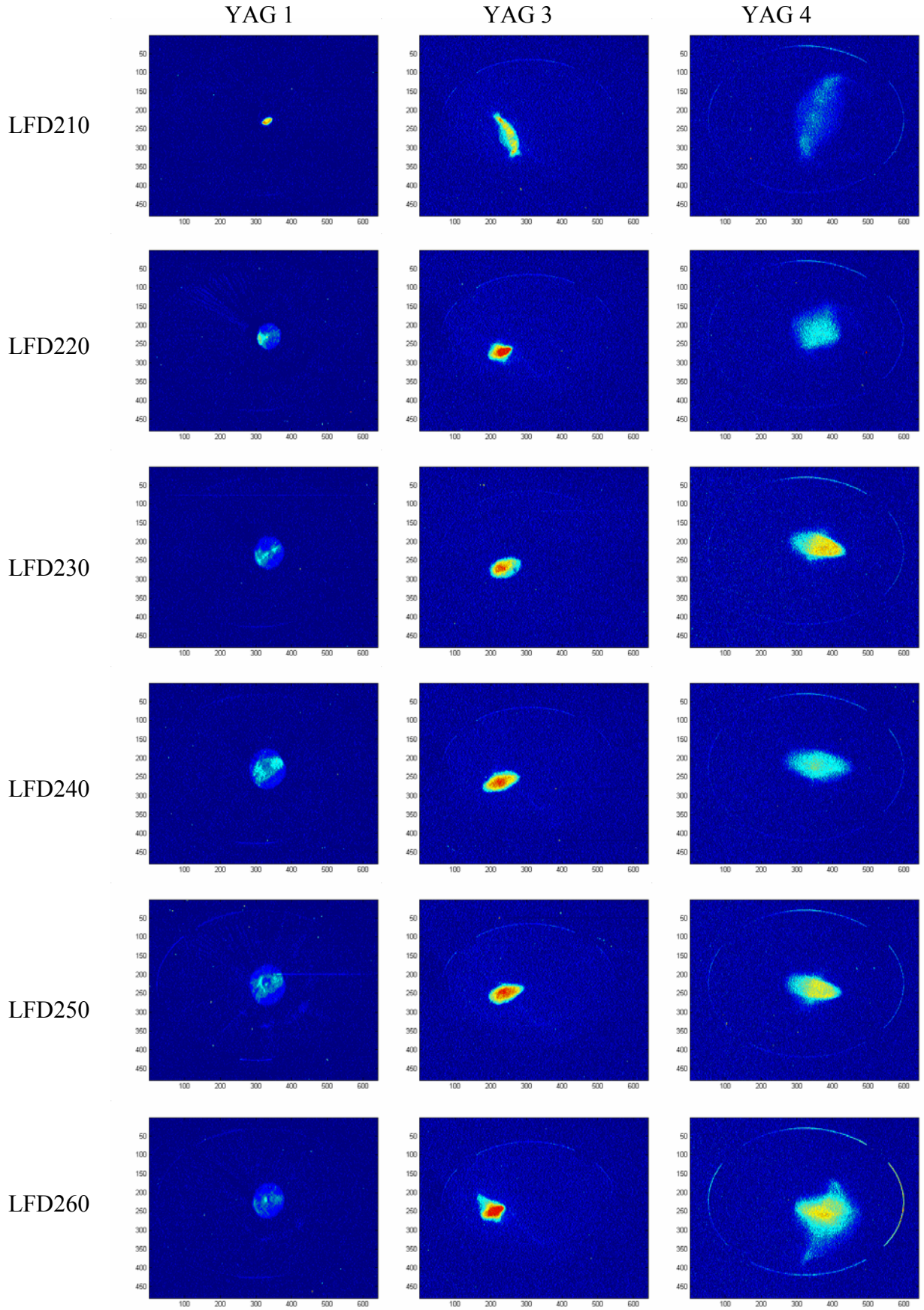


Fig. 2. Typical images of beam spots for the case of large laser spot size.

		rms. X (mm)	rms. Y (mm)	rms. R (mm)
LFD210	YAG 1	0.8078598	0.838383	0.8229799
	YAG 3	2.1541882	4.7534118	3.19996
	YAG 4	3.29067	8.4879559	5.2849846
LFD220	YAG 1	1.4173358	1.6992127	1.5518875
	YAG 3	1.7543684	2.0431579	1.8932648
	YAG 4	3.017231	3.4526301	3.227597
LFD230	YAG 1	1.8447785	2.3360858	2.0759482
	YAG 3	1.90855	1.9746	1.9412941
	YAG 4	3.1711468	2.3170344	2.7106561
LFD240	YAG 1	2.0081866	2.6524038	2.3079258
	YAG 3	2.2769845	2.0328621	2.1514635
	YAG 4	3.6440253	2.4183717	2.9686036
LFD250	YAG 1	2.1739002	2.861218	2.4939933
	YAG 3	2.12175	1.9622727	2.0404539
	YAG 4	3.3702648	2.5835996	2.9508329
LFD260	YAG 1	1.9376807	2.5609006	2.2276013
	YAG 3	2.1725444	2.1211765	2.1467068
	YAG 4	3.4982086	3.7259542	3.610286

Table 1. Rms. X (horizontal), rms. Y (vertical), and rms. R (geometric mean) of beam spots for different laser fine delay are listed.

If we compare the images in fig. 2 and data in table 1 with PARMELA simulation results, as shown in Fig. 3, we will find some similar phenomena. From LFD230 to LFD250, the shapes of beam spots look similar, and beam spot size are very close. When increasing or decreasing laser fine delay, beam starts to show the phenomenon of overfocusing. PARMELA simulation also confirms this phenomenon. At the range that initial RF phase equal to  $40^\circ$  -  $60^\circ$ , beam envelopes are very close, over the range obvious beam overfocusing can be found.

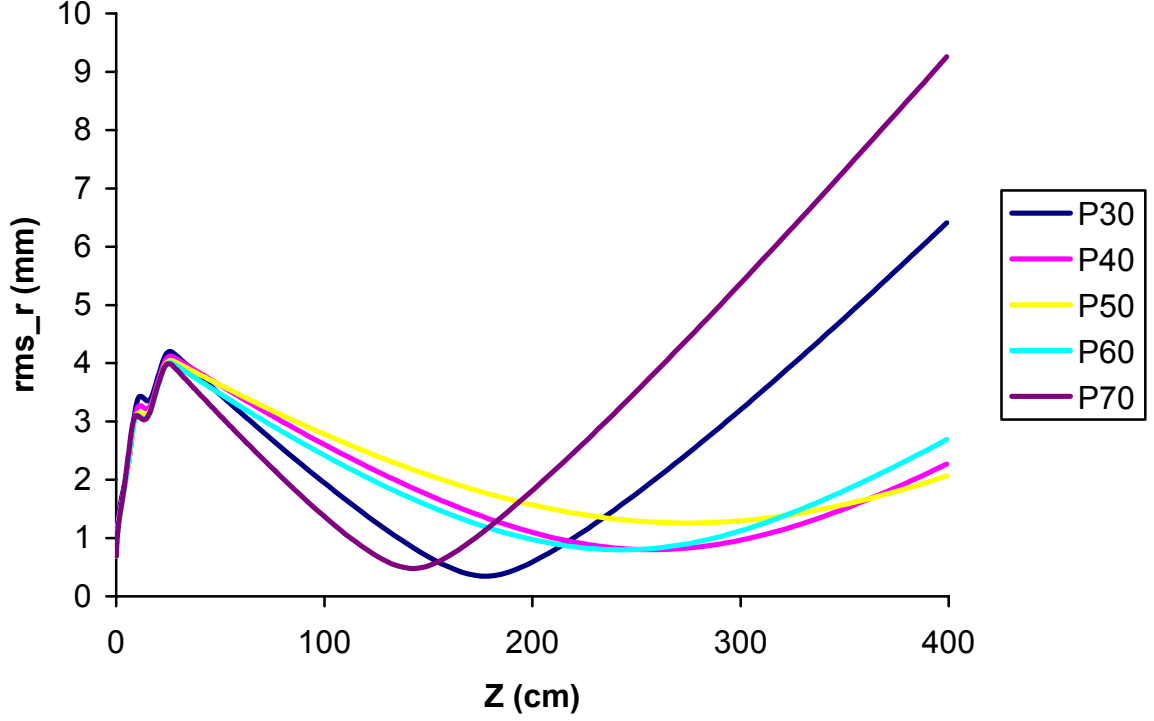
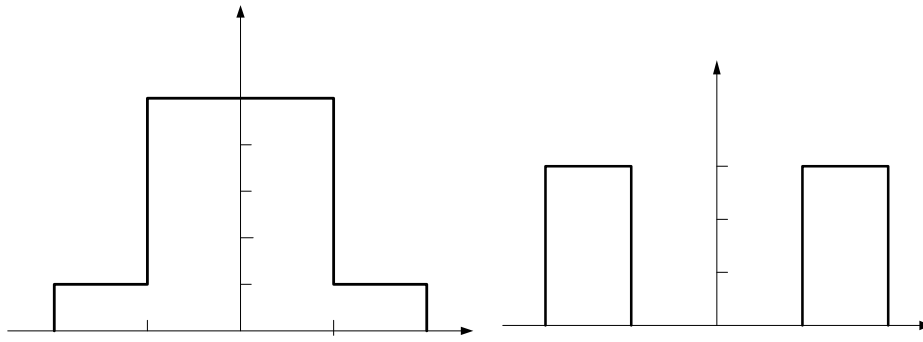


Fig. 3. Rms. beam envelopes along AWA test-stand beamline correspond to different initial RF phase of gun ( $\Phi=30^\circ - 70^\circ$ ), these curves are from PARMELA simulation for 1nC case.

The next step we will do is to simulate beam dynamics by using PARMELA at the same conditions as the measurement. If the rms. beam envelope obtained from the simulation can fit the measured data as shown in Table 1, we can say that the rms. transverse emittance of actual high-brightness beam approximately equals to the emittance we obtained from PARMELA simulation. Naturally the estimation is not exact. All the conditions we set in the simulation are ideal, the initial beam distribution is round, flat-top, and uniform, the RF gun and solenoids are azimuthally symmetry, no nonlinear effect exists, so the beam spot always keep round along the beamline. Actually our measurements showed that beam spots observed at YAG1, YAG3, and YAG4 look like ellipse, though laser spot hit on the photocathode is round. This indicates that some nonlinear effects existed in our beamline system distorted the beam shape. In order to make the estimation of actual emittance more believable, we choose to simulate two worst cases, one is called “hot spot”, and other is “cold spot”. The initial transverse distributions of particle density for the two cases are shown in Fig. 4 (a) and (b). The longitudinal distribution keeps uniform. It is impossible that actual beam distribution is worse than these two cases. As shown in Fig. 5 we will see the rms. envelope curves for the two cases can also fit the measured data, but the emittance are 3 or 4 times worse than ideal case, so we can obtain the worst emittance. The emittance from our actual beam should be in the range between the ideal case and the worst ones. We believe the estimation is more reliable.



(a) Hot spot

(b) Cold spot

Fig. 4. Transverse particle density profiles for (a) hot spot, (b) cold spot. For “hot spot”, particle density in the inner circle is 5 times more than the one in outer circle. “Cold spot” looks like a donut, particles distribute in the outer circle only.

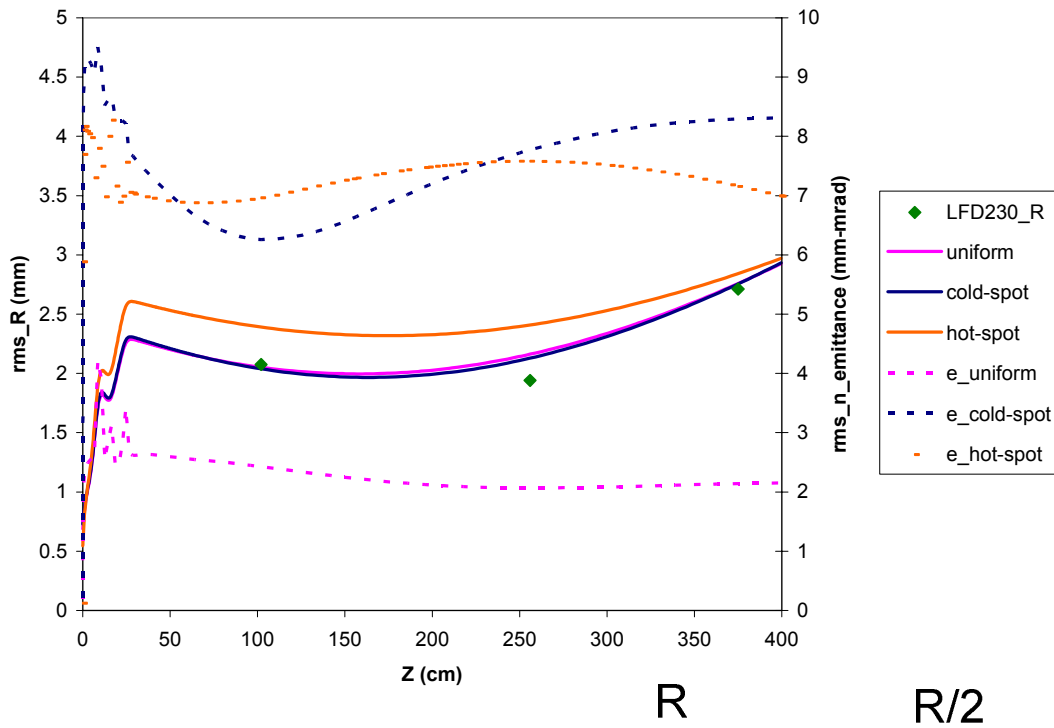


Fig. 5. PARMELA simulation fit the measured data. Dots express measured data, solid lines are rms. envelope from simulation, and dashed lines are normalized rms. transverse emittance for different cases.

In Fig. 5 we select one group of data (LFD230) used as comparison. Just as we mentioned above, beam spots are not round. To make the comparison more convenient, we made geometric mean for horizontal and vertical components of beam spots

( $\sigma_r = \sqrt{\sigma_x * \sigma_y}$ ). We simulated three cases, (a) uniform beam distribution, (b) hot spot, and (c) cold spot. The simulation conditions for all the cases are listed below.

$$\begin{aligned} Q &= 1\text{nC} \\ \Phi_{\text{rf}} &= 50^\circ \\ E_z &= 70\text{MV/m} \\ R_{\text{spot}} &= 1.425\text{mm} \end{aligned}$$

From the figure we found envelope curves for all the cases can fit the measured data, the cases of uniform distribution and cold spot match the measured data better. As shown by dashed lines, the emittance for uniform case is about 2 mm•mrad, for the case of “cold spot”, the emittance is around 8 mm•mrad. So we estimate that the emittance of actual beam from AWA test-stand beamline is in the range between 2 and 8 mm•mrad. Till now we finish analyzing the first group of data, we will continue data analyze in the next section.

## 2. Small laser spot size

The measurement conditions used for this case are

$$\begin{aligned} R_{\text{spot}} &= 1\text{mm} \\ R\bar{F}_{\text{gun}} &= 200\text{mV} \\ \text{TSF} &= \text{TSB} = 20000 \text{ counts} \\ \text{TSM} &= 24000 \text{ counts} \\ \text{ICT} &= 10\text{-}15\text{mV (for LFD233)} \\ \text{ICT} &= 15\text{-}20\text{mV (for LFD243)} \\ \text{ICT} &= 15\text{-}25\text{mV (for LFD253)} \\ \text{ICT} &= 15\text{-}20\text{mV (for LFD263)} \\ \text{ICT} &= 20\text{-}30\text{mV (for LFD273)} \end{aligned}$$

In this subsection we varied laser fine delay (LFD) from 233 to 273. The typical images of beam spots at YAG1, YAG3, and YAG4 are shown in Fig. 6, these images have been processed, and the background noises were removed. Table 2 shows rms. X (horizontal direction) and rms. Y (vertical direction) of beam spots for the three positions, since the measured beam spots were elliptic, not round, rms. R (geometric mean of rms. X and rms. Y) was calculated, and listed in the table for easy comparison to PARMELA simulation.



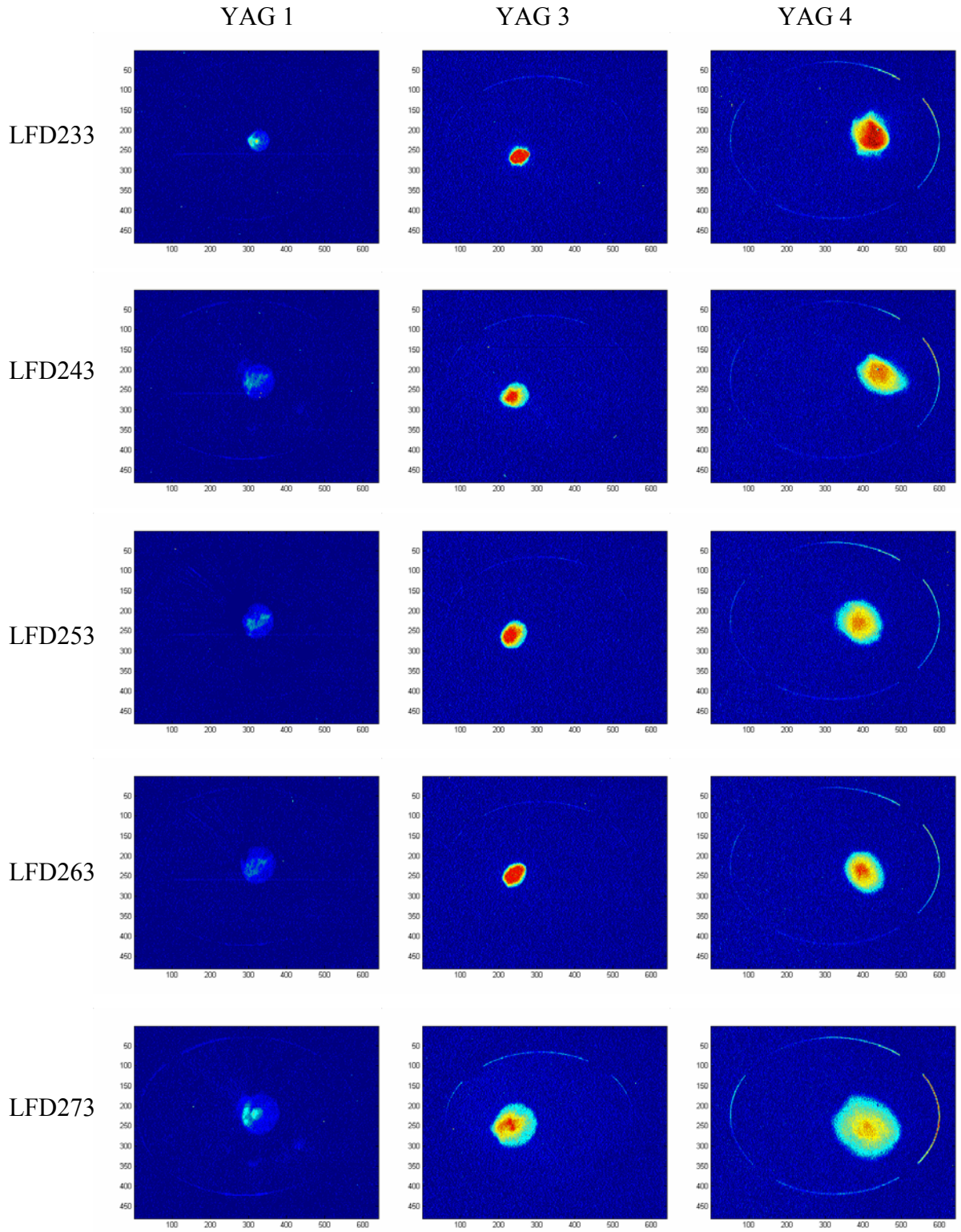


Fig. 6. Typical images of beam spots for the case of small laser spot size.



		rms. X (mm)	rms. Y (mm)	rms. R (mm)
LFD233	YAG 1	1.123528373	1.311752591	1.213998045
	YAG 3	1.219066667	2.1198	1.60753772
	YAG 4	1.958862725	3.345754322	2.560053403
LFD243	YAG 1	1.766808123	2.335662	2.031419847
	YAG 3	1.636887037	2.153666667	1.877580637
	YAG 4	2.400604703	3.039376219	2.701173976
LFD253	YAG 1	1.67385772	2.1272706	1.886994519
	YAG 3	1.5738875	2.349375	1.922927962
	YAG 4	2.36014165	3.13878116	2.721758282
LFD263	YAG 1	1.845610481	2.488213	2.142958701
	YAG 3	1.391646296	2.130777778	1.722001453
	YAG 4	2.127714441	2.954878647	2.507416593
LFD273	YAG 1	2.118841544	2.788437167	2.430690542
	YAG 3	2.451875926	3.38	2.878774154
	YAG 4	3.518999631	4.288273025	3.88464042

Table 2. Rms. X (horizontal), rms. Y (vertical), and rms. R (geometric mean) of beam spots for different laser fine delay are listed.

The next step we will do is to simulate beam dynamics by using PARMELA at the same conditions as the measurement. We also simulate three kinds of transverse beam profiles, (a) uniform distribution, (b) hot spot, and (c) cold spot. As shown in Fig. 7 we select one group of data (LFD243) used as the comparison. The simulation conditions for all the cases are listed below.

$$\begin{aligned}
Q &= 0.5\text{nC} \\
\Phi_{\text{rf}} &= 50^\circ \\
E_z &= 70\text{MV/m} \\
R_{\text{spot}} &= 1\text{mm}
\end{aligned}$$

From the figure we found envelope curves for all the cases can fit the measured data, the cases of uniform distribution and cold spot match the measured data better. As shown by dashed lines, the emittance of actual 0.5nC beam from test-stand beamline should be in the range between 1.3 and 4 mm•mrad.

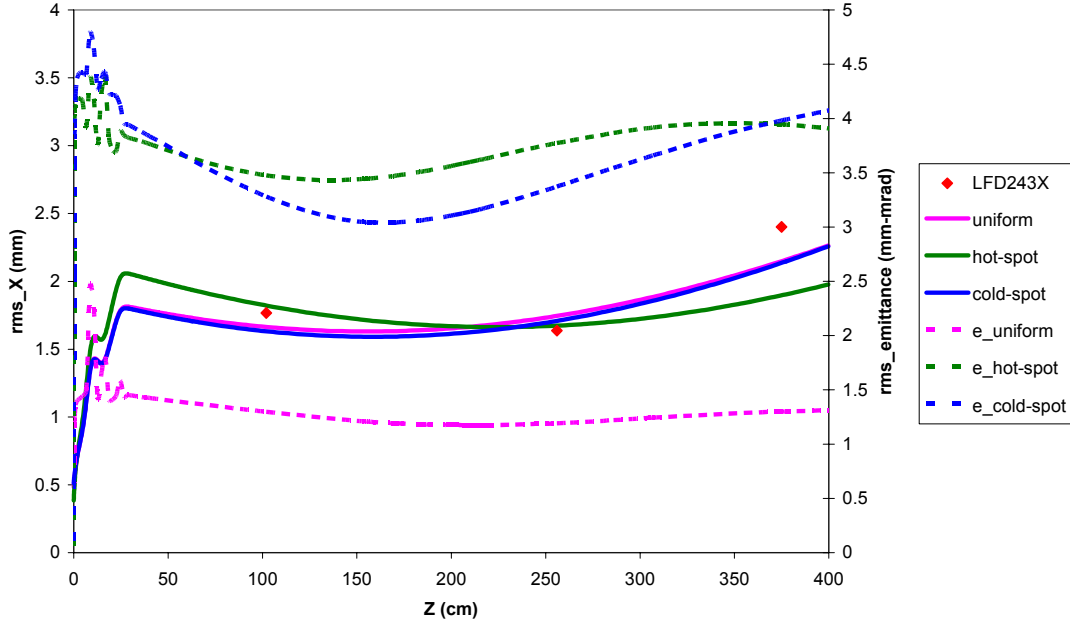


Fig. 7. PARMELA simulation fit the measured data. Dots express measured data, solid lines are rms. envelope from simulation, and dashed lines are normalized rms. transverse emittance for different cases.

### 3. High RF input power

In the group of measurements, we increased RF power. Correspondingly the solenoid fields were also increased. The detailed measurement conditions used for this case are

$R_{\text{spot}}=1.425\text{mm}$   
 $RF_{\text{gun}}=230\text{mV}$   
 $ICT=30\text{mV}$  ( $Q=0.8\text{nC}$ )  
 $LFD=250$   
 $TSB=24190$  counts  
 $TSF=24630$   
 $TSM=26829$  counts (for data “WGbest”)  
 $=28149$  counts (for data “WGbest\_C”)

The typical images of beam spots at YAG1, YAG3, and YAG4 are shown in Fig. 8, these images have been processed, and the background noises were removed. Table 3 shows rms. X (horizontal direction) and rms. Y (vertical direction) of beam spots for the three positions, since the measured beam spots were elliptic, not round, rms.R (geometric mean of rms. X and rms. Y) was calculated, and listed in the table.

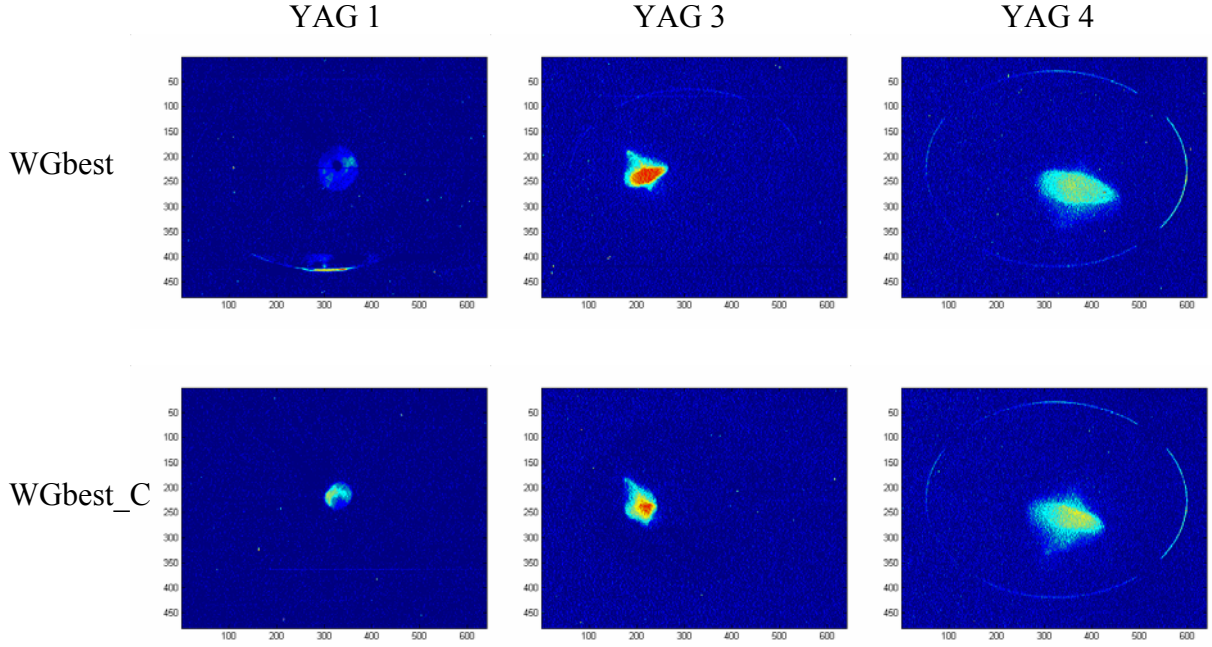


Fig. 8. Typical images of beam spots for the case of high RF input power.

		rms. X (mm)	rms. Y (mm)	rms. R (mm)
WGbest	YAG 1	1.817256022	2.542085	2.14932996
	YAG 3	1.977146154	2.218615385	2.094403704
	YAG 4	3.468866516	2.739532321	3.082705295
WGbest_C	YAG 1	1.280614262	1.323231	1.301748244
	YAG 3	2.261938462	3.055384615	2.628895581
	YAG 4	3.225262856	2.896830611	3.056638704

Table 3. Rms. X (horizontal), rms. Y (vertical), and rms. R (geometric mean) of beam spots for “WGbest” and “WGbest\_C”. The only difference of these two cases is data “WGbest\_C” have higher matching solenoid field (TSM).

## Summary

We chose three positions along AWA test-stand beamline, and measured beam spots at different conditions. PARMELA simulation was done at the same conditions as the measurement. In the simulation we consider three kinds of beam profiles, one is uniform, and another two are “cold spot” and “hot spot”. The rms. envelope curves from all the three cases can fit the data, but they have large difference of rms. transverse emittance. From the comparison we can estimate that the emittance of actual 1nC beam from AWA test-stand beamline is in the range between 2 and 8 mm•mrad.